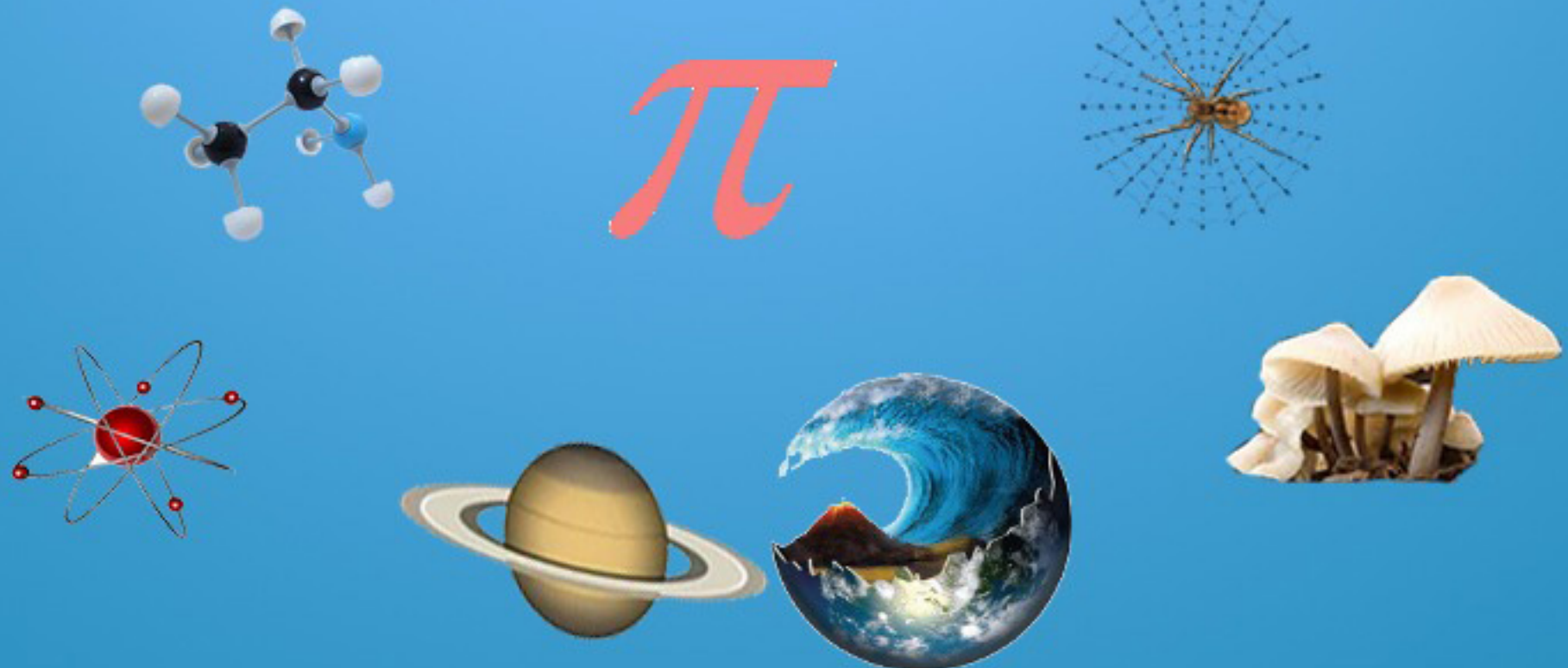


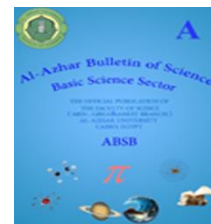
A

Al-Azhar Bulletin of Science Basic Science Sector

THE OFFICIAL PUBLICATION OF
THE FACULTY OF SCINCE
(MEN , GIRLS & ASSUIT BRANCH)
AL-AZHAR UNIVERSITY
CAIRO, EGYPT

ABS





MODELING OF THE DYNAMICS ADSORPTION OF SOME HAZARDOUS ELEMENTS FROM AQUEOUS SOLUTION ONTO BENTONITE-CALCIUM-ALGINATE BEADS

Riham Abdel-Kareem Abou-lilah^{a*}, Hoda El-Sayed Rizk^{*}, Mostafa Elshorbagy^{*}, Azza Mohamed Gamal, Amal Mohamed Ali^{*} and Nagwa Badawy

Chemistry Department, Faculty of Science, (Girls), Al-Azhar University, Cairo, Egypt.

* Hot Laboratories and Nuclear fuel technology, Atomic Energy Authority, Cairo, Egypt.

a^{*} : Corresponding Author: Ri roka@yahoo.com.

Received: 28 Dec 2020; Revised: 06 Jan 2021; Accepted: 09 Jan 2021; Published: 4 Oct 2021

ABSTRACT

Encapsulation of bentonite-Ca-alginate was employed for discharge of Cs^+ , Sr^{2+} , UO_2^{2+} and Co^{2+} from aquatic solution. Preferable pH for elimination of these ions was 5.5. For radiation stability, bentonite-Ca-alginate was investigated; a ^{60}Co source was used to expose it to gamma radiation. Data obtained from (FT-IR) assessed radiation-induced effect on a stability of bentonite-Ca-alginate. Irradiated samples until 100 kGy do not impair an absorption of an ions examined. In a column application, bentonite-Ca-alginate composite beads were examined for the discharge of these ions from multicomponent solution using fixed-bed column. Effect on column output of various parameters, like bed height, flow rate and initial inlet concentration were investigated. The column performance was 49, 46, 47 and 46.6% for Cs^+ , Sr^{2+} , UO_2^{2+} and Co^{2+} , respectively at flow rate of 0.5mL/min, 3cm bed depth and initial metal concentration, 50mg/L for each element. Thomas and Yoon-Nelson models identified a breakthrough curves, which successfully predict breakthrough adsorption curves.

Keywords: Alginate; Column modeling; Gamma radiation.

1. INTRODUCTION

From point view of health, nuclear waste dumping has a significant concern. Environmental contamination is induced by toxic emissions emanating from operation and maintenance of nuclear power plants, nuclear weapons testing, and nuclear medicine. Huge quantities of radioactive products, like Cs^+ , Sr^{2+} , UO_2^{2+} and Co^{2+} , have been released into the environment, resulting in significant pollution of surface water and soil particles. Cesium (^{137}Cs) enhanced as a consequence of nuclear accident is considered one of environmental precarious elements because of its half-life (30.4 years). Among the most prevalent radionuclides found in radioactive liquid waste (LRW) is strontium-90, that can easily replace calcium and cause leukaemia, anaemia and other diseases when it reaches the

human body. Uranium can get in an environment through the extraction, processing and use of uranium, causing hazards to the ecological environment and human health as a consequence of chemical toxicity and radioactivity [1]. ^{60}Co is considered among the most extreme environmental radionuclides. Several health problems can be produced from higher cobalt concentrations [2-3]. In recent centuries, a major interest has been dedicated to looking for environmentally friendly, sustainable and low-cost technologies for pollutants removal from wastewater. Bentonite belongs to the group of clay minerals which are layered structures with large surface area, high capacity (CEC), and good chemical and mechanical stability that predispose them as good adsorbent [3]. Bentonite cannot be directly applied in fixed-bed columns because

Journal Homepage: <https://absb.journals.ekb>

they lead to blocking the column. A revolutionary alginate microcapsule enclosing bentonite was developed for removing these ions from multicomponent solution to resolve the aggregation for bentonite clay flacks in column. [4]. Therefore, Wastewater care should be established to block these contaminants risk on an environment and public health. Hence, this work focused on using the encapsulating bentonite-Ca-alginate as a sorbent material for discharge of Cs^+ , Sr^{2+} , UO_2^{2+} and Co^{2+} from multicomponent solution utilizing a fixed-bed column. Impact of significant parameters, including impact of bed depth, flow rate, and concentration of metal ions, was inspected and compared with Thomas and Yoon-Nelson model predictions. Zero point charge detection of sorbent material was analyzed. It investigated gamma irradiation impact on structure and a removal efficiency at $25 \pm 1^\circ\text{C}$ of sorbent used.

2. EXPERIMENTAL

2.1. Materials

All reagents are of analytical quality and without cleansing further. Cobalt nitrate, Calcium chloride and sodium alginate with purity 99.8% were purchased from Prolabo Pure Chemical Ind. Cesium nitrate and Strontium chloride of purity 99.9% were purchased from Fluka. Uranyl nitrate, $\text{UO}_2(\text{NO}_3)_2 \cdot 6\text{H}_2\text{O}$, of purity equals 98% was bought from BDH. The solution's pH was adiusted, using HCl and/or NaOH which were purchased from Porlabo, using CG-820 Schott Gerate pH meter, Germany, of accuracy ± 0.01 . Double-distilled water was utilized for all tests.

2.2. Bentonite-alginate Preparation

Bentonite-Ca-alginate composite was synthesized and characterized confirming to the procedure described in a previous work Abou-Lilah et al. [4]. Preparation of dissolved bentonite suspension was a first stage. Bentonite suspension sample was combined with a 3 percent NaALG solution for around 2 hours by a high speed agitator. An obtained sol was dropped wise into 2% CaCl_2 solution out of a 0.3-mm medical needle. The formed pellets were gently stirred in the CaCl_2 solution for 3 h to get hardened, and then they were separated, three folds washed with pure water, and dried at $40 \pm 1^\circ\text{C}$ for 24h. Identification of synthesized composite was confirmed in the

previous work [4]. Bentonite-Ca-alginate surface is loose in the SEM picture and uniform with modest porosity. Further, the loading of alginate on bentonite is very clear. FT-IR spectra demonstrated the characteristic peak of bentonite-Ca-alginate which clarifies that almost all peaks of the raw bentonite exist in the bentonite-Ca-alginate spectrum, with some considerable shifts. This result attributed to that the reaction merely through some ion exchange (IX) mechanisms. Those IX reactions protect the pattern and the main occupational groups of bentonite and alginate [5].

2.3. Adsorption Studies

An optimum pH value for discharge of $50 \pm 1\text{mg/L}$ Cs^+ , Sr^{2+} , UO_2^{2+} and Co^{2+} from multicomponent solution using bentonite-Ca-alginate gel beads was examined in a range from 1-7 and adjusted by a few drops of dilute NaOH or HCl by pH meter of accuracy ± 0.01 . Sorbent Removal efficiency before and after irradiation to different γ -radiation doses was investigated. Experiments were accomplished in glass bottles containing equal volumes, 5 ± 0.05 mL, of 50 ± 1 mg/L Cs(I), Sr(II), U(VI) and/or Co(II) ions solutions in aqueous medium with 0.05 g bentonite-Ca-alginate. Bottles were capped and agitated with a mechanical shaker at room temperature. Samples were gathered at the expected equilibrium and their concentrations were calculated. Initial and final concentrations of Cs(I), Co(II) and Sr(II) ions in liquid phase were determined after phase separation by centrifugation using (AAS). Initial and final uranium ion concentration was analysed using a standard Arsenazo (III) [6] using Shimadzu UV-vis spectrophotometer model UV-160A, Japan. Uptake was computerized from a following equation [7]:

$$\text{Uptake} = \frac{\text{C}_o - \text{C}_e}{\text{C}_o} \quad (1)$$

Where C_o and C_e are concentrations from each metal ions in initial and final solutions, respectively. Zero point charge of bentonite-Ca-alginate was defined by shaking a series of 50 mL bottles containing 0.1g of the granulated composite and 10 mL from 0.1M NaCl its pH was varied from 1 to 11 using 0.1M HNO_3 and 0.1M KOH for 24h at room temperature. The final recording supernatant pH was noted, and efficiency of the removal after irradiating sample to different γ -radiation doses.

2.4. Column Studies

A glass column of 10.0 cm in length and 1.0 cm in inner diameter packed with bentonite-Ca-alginate beads, to overcome the aggregation for bentonite clay flask as a fixed bed column and supplied with a constant-flow changeable speed peristaltic pump for the discharge of Cs^+ , Sr^{2+} , UO_2^{2+} and Co^{2+} in multicomponent solution. Before an adsorption process, the column was conditioned with bidistilled water for approximately 20 min. Impacts of process parameter such as different total metal ions concentrations (200, 400, and 800 mg/L), bed depth (3, 6, and 8 cm) and flow rates (0.5, 1.5, and 2 mL/min) at optimum pH were studied. Effluents were sampled at intervals and analyzed using AAS (Buck scientific model VGP 210) (for Cs(I), Co(II) and Sr(II)) and a Shimadzu, UV/visible recording spectrophotometer type UV-160A (for uranium). In addition, total adsorbed quantity for a component i ($q_{\text{total},i}$, mg) calculated as follows [8]:

$$q_{\text{tot}} = \frac{Q}{1000} \int_{t=0}^{t=\text{tot}} C_{\text{ads}} dt = \frac{Q}{1000} \int_{t=0}^{t=\text{tot}} (C_o - C) dt \quad (2)$$

Where Q is a flow rate, mL/min, t is time, min, t total is a total time for a column to be saturated, min, $C_{o,i}$ and C_i are inlet and outlet concentrations (mg/ L) of a component i, respectively. Also, an effluent volume (V_e , mL) that is a solution volume passed through column in time t_e is computed as follows:

$$V_{\text{eff}} = Q \times t_{\text{eff}} \quad (3)$$

The maximum column adsorption capacity ($q_{\text{max},i}$) calculated by dividing a quantity of adsorbed ions ($q_{\text{total},i}$) by mass of bentonite-alginate in the bed (g) [9].

Total amount for component i sent to a column ($m_{\text{total},i}$, mg) the removal percent (column performance), R_i , of a component i and the total removal percent (R_{total}) for multicomponent solution computed as follow[10-12]:

$$m_{\text{tot}} = C_o \frac{V_{\text{eff}}}{1000} \quad (4), R_i = \frac{q_{\text{total},i}}{m_{\text{total},i}} \quad (5),$$

$$R_{\text{total}} = \frac{\sum q_{\text{total},i}}{\sum m_{\text{total},i}} \quad (6)$$

3. RESULTS AND DISCUSSION

3.1. Determination of charge at zero point

That pH from which zero value was taken from sorbent surface charge is known as the zero charge point (pHzpc). A charge of a positive surface sites equals that of negative ones at this pH. A pHzpc information helps us to hypothesize an ionization of functional groups and their interaction with metal forms in solution; a sorbent surface is negative in a charge with solution pHs higher than pHzpc which could communicate with positive metal species, while solid surface is positively charged at pHs smaller than pHzpc and could communicate with negative species [13-16]. ZPCs of bentonite-Ca-alginate was calculated by plotting $\Delta p\text{H}$ versus initial pH, a pH curve intersected at a point that gave zero point charge of 8 for bentonite-alginate as illustrated in Fig. (1).This result is in agreement with the value obtained by Dong-Su Kim [17].

3.2. pH Studies

PH Influences of a removal efficiency, Eq. (2), of 50 ± 1 mg/L of Cs^+ , Sr^{2+} , UO_2^{2+} and Co^{2+} onto 0.05 g of bentonite-Ca-alginate was studied from 1 to 7, Fig. (2). It's possible to see that sorption of Cs^+ , Sr^{2+} , UO_2^{2+} and Co^{2+} onto bentonite-Ca-alginate is markedly pH-dependent. It is evident that uptake was low at lower pH for all investigated ions. This is clarified by the competition of protons for sites on the sorbents at lower pH which the surface become less negative owing to an existence excess of H^+ protons. Values of uptake were raised with increasing initial pH value, this attributed to that a positive charge decreases on a surface as pH increases, and this would cause lower repulsion of the adsorbed ions [18]. The higher removal efficiency values were occurred at initial pH of 5-6. The next experiments carried out at pH 5.5. Maximum sorption capacities of modified bentonite were accomplished at lower values of ZPC (8). This results because of second type of surface functional groups on montmorillonite interacting with cations are structural-charge surface sites (substitution of Al^{3+} for Si^{4+} within the tetrahedral surface layer) [19]. Surface Sites of Structural-charge carry a permanently negative charge to isomorphic substitutions in tetrahedral and octahedral layers and independent on pH [17]. This sort of sites,

hereinafter pointed to as X layer sites, lead rise to the exchange capacity observed in clay minerals. Their chemical reactivity is mainly due to ion exchange reactions occurring at these sites.

3.3. Impact of gamma irradiation on sorption behavior

3.3.1. Fourier transforms infrared spectroscopy

Gamma irradiation effects on a structure of bentonite-Ca-alginate was estimated by irradiating the sample to ^{60}Co gamma source, up to radiation doses of 25, 50, and 100 kGy, respectively. Fig. (3), illustrated impact of dose exposure on a surface functional groups of an irradiated patterns which indicates there is slightly difference between original and irradiated samples and the radiation-induced raise in intensity of several of the peaks present including those at $3600\text{-}3200\text{cm}^{-1}$, 1600cm^{-1} and 1000cm^{-1} for bentonite-Ca-alginate since the bands increase at 25kGy, decreased at 50kGy and then increased again at 100kGy. This alteration in an intensities of these bands could be utilized to monitor a mentioned ions loading of bentonite-Ca-alginate and though the applicability of this concept would have to be

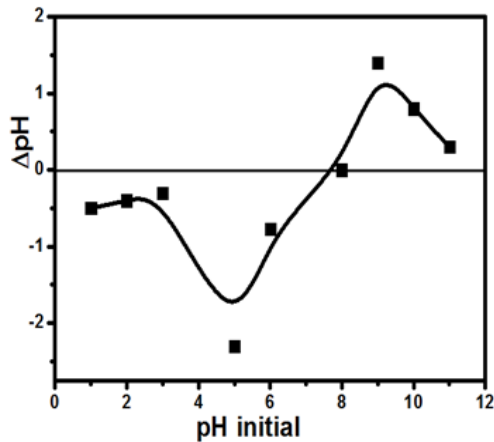


Fig. 1. Zero point charge of Bentonite-Ca-alginate.

studied further as is postulated by Zhaoyi et al [20].

3.3.2. Impact of gamma irradiation on a sorbent's removal efficiency

Removal efficiency of origin and irradiated bentonite-Ca-alginate for Cs^+ , Sr^{2+} , UO_2^{2+} and Co^{2+} at optimum conditions are given in Fig.(4). The findings suggested that irradiated samples until 100 kGy has a marginal influence on an uptake of four ions. This result as that obtained by Holdsworth et al. on Cs^+ uptake [21]. There are slightly raise in a removal efficiency after irradiation due to γ -irradiation causes partial reduction of trivalent iron to a divalent state due to hydrogen radicals production from a radiolysis of interlayer water which increase uptake as reported by Gournis et al [22].

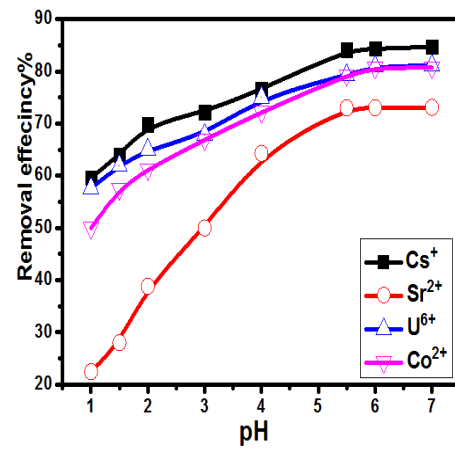
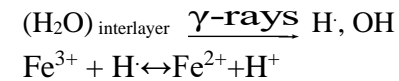


Fig. 2. Effect of pH on the removal efficiency of Bentonite-Ca-alginate.

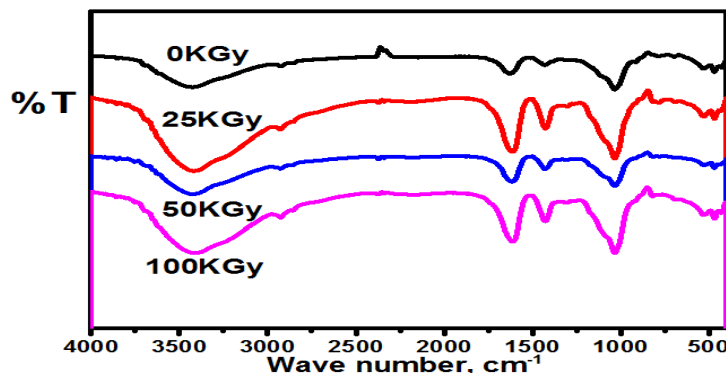


Fig. 3. FTIR spectra of original and irradiated Bentonite-Ca-alginate.

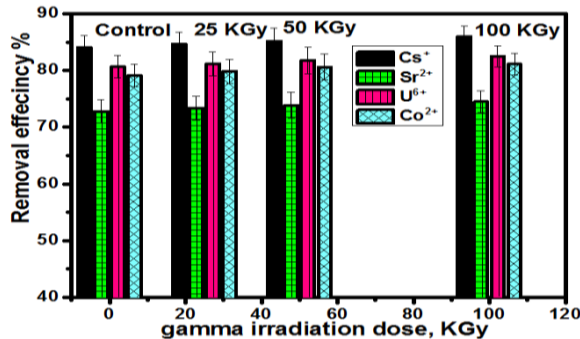


Fig. 4. Effect of gamma radiation on the removal efficiency of bentonite-Ca-alginate.

3.4. Column studies

Parameters such as bed height, flow rate, and initial inlet concentration are important in column design. Their influence on shape of breakthrough curve of column adsorption operation for of Cs^+ , Sr^{2+} , UO_2^{2+} and Co^{2+} adsorption from multicomponent solution onto modified bentonite (bentonite-Ca-alginate composite beads) at pH 5.5 were investigated.

3.4.1. Influence of initial inlet concentration

Impact of various initial concentrations of an influent on column performance of bentonite-Ca-alginate composite beads at constant other experimental condition, flow rate of 0.5 mL/min, bed depth of 3.0 cm and pH of 5.5, was examined by varying ion concentrations 50-200mg/L from each ion. Fig. (5(a-d)), illustrated that when a total initial concentration of an influent increased from 50-200 mg/L, breakthrough time decreased. However, as seen in the Table (1), values of q_{total} , and the breakthrough adsorption capacity increased. This behavior demonstrated that a change of concentration has significant affects the saturation rate and breakthrough time [23]. This could be because of that a possibility of a greater number metal ions number in solution and more adsorption sites of bentonite-Ca-alginate sorbents were being covered at higher impact concentration and lower concentration gradient between liquid and solid phases caused slower transport that a decreased coefficient of mass transfer [24]. Breakthrough curves are sharper, steeper and shifted to an origin for metal ions with used sorbent with rising influent concentration because an active sites of bentonite-Ca-alginate fixed-bed system is saturated more rapidly at higher initial concentrations, time to reach both a

breakthrough and exhaustion point is decreased [25-26]. Amount of Cs^+ , Sr^{2+} , UO_2^{2+} and Co^{2+} ions adsorbed in a multicomponent system was found to increase with rising an initial concentration of metal ions from 50 to 200 mg/L however, column performance decreased, as recorded in Table (1). Increasing influent concentration caused treated effluent volume and total mentioned ions removal to decrease. [25, 12, 27].

3.4.2. Effect of bed depth

Breakthrough curves of bentonite-Ca-alginate was operated at different bed depths (3.0, 6.0, and 8.0 cm) at constant influent concentration of Cs^+ , Sr^{2+} , UO_2^{2+} and Co^{2+} mixture equal 50mg/L from each metal ions, flow rate of 0.5 mL/min and pH 5.5. Generally, breakthrough time and the exhaustion time for the investigated ions adsorption are raised with increasing a bed depth from 3 to 8 cm as illustrated in Fig. (6(a-d)) as is confirmed in literature [28]. Data in Table (2) demonstrated that as the height of adsorption mass increase the adsorption capacity increase however, slope of breakthrough curve decreases this behavior as a consequence of an increase in a surface area of sorbent which, availability of more active site increase [29]. A higher height of bed reveals a larger amount of adsorbent residing in the column, which suggests that there are also further binding sites accessible. The time for a metal ions to disperse through an entire material bed is not adequate at a lowest bed height, allowing a shorter breakthrough time to occur. [30-32, 12].

3.4.3. Flow rate Impact

Feed flow rate is one of an important parameters that could affect retention capacity in fixed-bed experiments, especially for a continuous process at a manufacture scale [33].The influence of flow-rate on retention for component (Cs^+ , Sr^{2+} , UO_2^{2+} and Co^{2+}) onto bentonite-Ca-alginate composite adsorbents in a column from multicomponent solution was investigated about various flow rates from 0.5 to 2.0 mL/min with a bed depth 3.0 cm, C_0 of 50 mg/L of each ion and pH of 5.5. Fig. (7(a-d)) illustrated breakthrough curves at different flow rates for Cs^+ , Sr^{2+} , UO_2^{2+} and Co^{2+} adsorption from multicomponent solution. At higher influent rate, ions had short time to be in contact with adsorbent, in which led to a lower

uptake for an influent ions in column with ultimately shortened breakthrough time and exhaustion time [34-36, 30]. Amount of component i ($q_{\text{total},i}$, mg) adsorbed can be detected by numerical integration of an area under a curve as defined in Eq(6). Rising flow-rate from 0.5 to 2.0 mL/min, a breakthrough time reduced, hence a relation is inversely, suggesting a longer column life with a longer contact time. Accordingly, from data in Table (3), and the corresponding breakthrough capacity is effected by the rate of flow rate of the influent. As a result a total amount of adsorbed ions, q_{total} , also decreased as the flow rate increased. The possible explanation may be that, at higher flow rates, the contact time between the metal ions and an active sites at an internal and external surfaces of an adsorbent is too short, resulting in a decrease in an adsorption capacity and removal efficiency of an investigated ions and, conversely, a low influx flow rate [12]. From Eq. (6) it has the capacity to calculate and record a total removal percentage of a multicomponent solution of four ions in a multicomponent system in Table (6). Total quantity adsorbed of four ions in multicomponent system can be computed by sum of quantity adsorbed from each metal ion. Curves of steep breakthrough were noticed at higher flow rates, which caused breakthrough time and exhaustion to occur earlier. At lowest flow rate of 0.5 mL/min, both highest ions uptake and highest bed retention capacity at breakthrough is obtained (Figures. (5-7) and Tables (1-3).

3.5. Dynamic adsorption models for Column Studies

Breakthrough curve modelling explains the efficiency of a fixed-bed column process and a promising concept that is required for expectation of a time-of-concentration profile and retention capacities under different operating conditions Below, two simple models are described, Thomas and Yoon-Nelson models.

3.5.1. Thomas model

Thomas model [37] suppose plug flow manner in bed and employs second-order reversible reaction kinetics and Langmuir isotherm for equilibrium [35]. This model is acceptable for adsorption procedures where no constraints on external and internal diffusion

exist and for a breakthrough curves expectation. A following equation describes linear form of Thomas model:

$$\ln\left(\frac{C_i}{C_o} - 1\right) = \frac{mq_{\text{Th},i}k_{\text{Th},i}}{Q} - C_o k_{\text{Th},i} t \quad (7)$$

Where $k_{\text{Th},i}$ is a Thomas kinetic coefficient (mL/min.mg) for component i and $q_{\text{Th},i}$ is an adsorbed quantity for component i (mg/g). Thomas parameters k_{Th} and q_o could be estimated from slope and intercept of the plot between $\ln((C_o / C_t) - 1)$ against t , respectively [38-39]. Fig. (8(a-d)) Displayed a Thomas models and a model parameters along with correlation factors and represent in Table (4) for bentonite-Ca-alginate. Values of q_{Th} raise with increasing influent concentration and bed depth [40]. This behavior may be clarified by a high concentration of influence causes an increased driving force for a mass transfer and enhances value of capacity and high bed depth provide high retention active sites and longer contact time [41-42, 38, 33]. In contrast, as an adsorption and diffusion times are declined by increasing flow rate, values of capacity are reduced. Otherwise, a values of Thomas rate constant, k_{Th} decreases with rising flow rate and influent concentration but increased with rising bed depth. A good linear correlation factor, R^2 (ranging from 0.91-0.98 for Cs(I), Sr(II), U(VI) and Co(II) retention from multicomponent solution onto bentonite-Ca-alginate indicates the good fitting of Thomas model with experimental breakthrough curve [43].

3.5.2. Yoon-Nelson model

A basic theoretical model developed by Yoon-Nelson. This model is based on an assumption that a rate of reduction in a possibility for adsorption for any adsorbate molecule is relative to a possibility for adsorbate adsorption and adsorbate adsorbent breakthrough [44]. This model was utilized to investigate breakthrough behavior of Cs^+ , Sr^{2+} , UO_2^{2+} and Co^{2+} in multicomponent solution on bentonite-Ca-alginate. Yoon-Nelson linear form equation is formulated as follows:

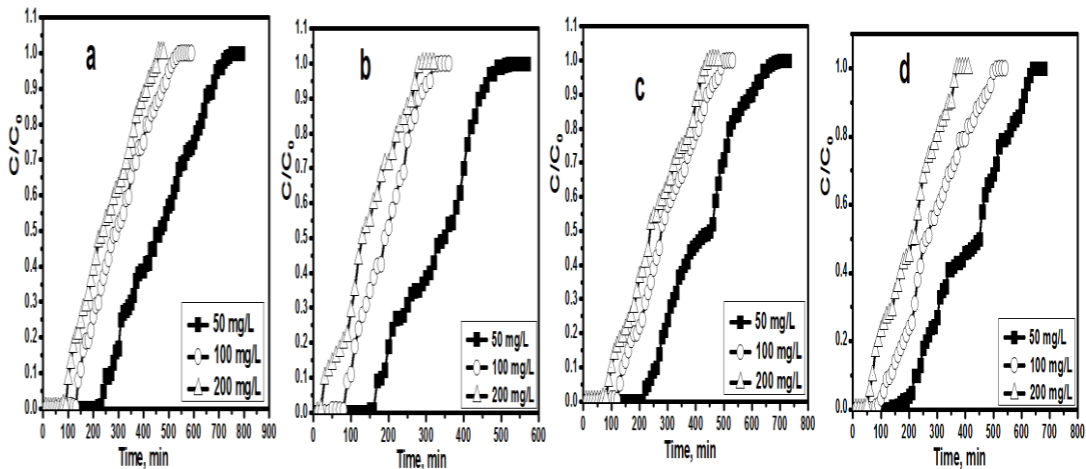


Fig. 5. Effect of metal ion concentration on the breakthrough curve for (a) Cs^+ , (b) Sr^{2+} , (c) UO_2^{2+} and (d) Co^{2+} onto bentonite-Ca-alginate at $\text{pH}=5.5$, flow rate = 0.5 mL/min and bed depth 3 cm.

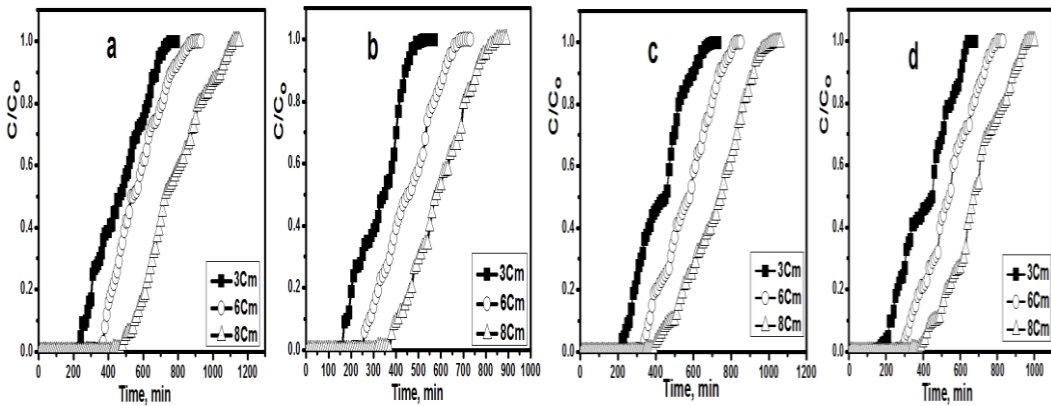


Fig. 6. Effect of bed depth on the breakthrough curve for (a) Cs^+ , (b) Sr^{2+} , (c) UO_2^{2+} and (d) Co^{2+} onto bentonite-Ca-alginate at $\text{pH}=5.5$, metal ion concentration of 50 mg/L form each element and flow rate=0.5mL/min.

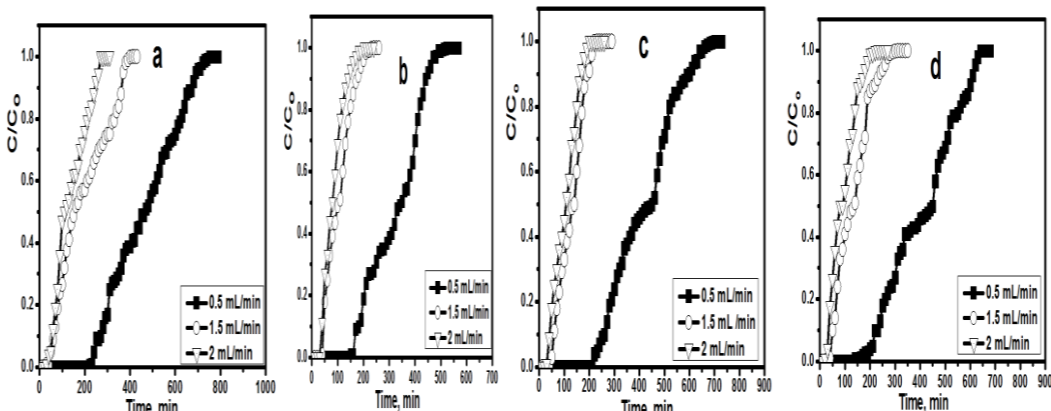


Fig. 7. Effect of flow rate on the breakthrough curve for (a) Cs^+ , (b) Sr^{2+} , (c) UO_2^{2+} and (d) Co^{2+} onto bentonite-Ca-alginate at $\text{pH}=5.5$, metal ion concentration of 50 mg/L of each ion and bed depth 3 cm.

Table 1. Breakthrough capacity, total quantity sorbed, and Column performance for sorption of Cs⁺, Sr²⁺, UO₂²⁺ and Co²⁺ by encapsulated bentonite-Ca-alginate at bed depth of 3 cm, flow rate of 0.5 mL/min and different metal ion concentrations.

Metal ion	Concentration, mg/L	Capacity, mg/g	q _{total} , mg	m _{total} , mg	Column performance, %
Cs ⁺	50	22.5	18.52	37.8	49
	100	27.1	22.4	55	44
	200	43	25	64	39
Sr ²⁺	50	16.6	14.5	31.5	46
	100	19	17	42.5	40
	200	32	20	55.6	35
UO ₂ ²⁺	50	20	16	34	47
	100	33	18.5	44	42
	200	40	21	56.8	37
Co ²⁺	50	19.4	15.6	33.4	46.7
	100	31.6	17.8	43.4	41
	200	39	20.6	56.7	36.3

Table 2. Breakthrough capacity, total quantity sorbed and column performance for sorption of Cs⁺, Sr²⁺, UO₂²⁺ and Co²⁺ (50mg/L form each element) by encapsulated bentonite-Ca-alginate at flow rate of 0.5 mL/min and different bed depths.

Metal ion	Bed depth, Cm	Capacity, mg/g	q _{total} , mg	m _{total} , mg	Column performance, %
Cs ⁺	3	22.5	18.52	37.8	49
	6	23	25	43.1	58
	8	24.1	29	43.7	66.3
Sr ²⁺	3	16.6	14.5	31.5	46
	6	17.5	16.2	32.2	50.3
	8	18	19	35	54
UO ₂ ²⁺	3	20	16	34	47
	6	22	19.3	36	53.6
	8	23.2	21	34.4	61
Co ²⁺	3	19.4	15.6	33.4	46.7
	6	21.3	18.1	34.3	52.7
	8	22.7	19.7	33.4	59

Table 3. Breakthrough capacity, total quantity sorbed and column performance for sorption of Cs⁺, Sr²⁺, UO₂²⁺ and Co²⁺ (50 ppm form each element) by encapsulated bentonite-alginate at bed depth of 3 cm and different flow rates.

Metal ion	Flow rate, mL/min	Capacity, mg/g	q _{total} , mg	m _{total} , mg	Column performance, %
Cs ⁺	0.5	22.5	18.52	37.8	49
	1.5	10.6	9.6	21.3	45
	2	7.3	7.8	19.8	39.3
Sr ²⁺	0.5	16.6	14.5	31.5	46
	1.5	7.6	8.2	20.5	40
	2	4.4	4.7	14.2	33
UO ₂ ²⁺	0.5	20	16	34	47
	1.5	9.3	9.8	23.3	42
	2	6.5	7	19.4	36
Co ²⁺	0.5	19.4	15.6	33.4	46.7
	1.5	9	9.2	23	40
	2	5.9	5.7	16.6	34.3

$$\ln\left(\frac{C_i}{C_0 - C_i}\right) = k_{YN,i}t - k_{YN,i}\tau_i \quad (8)$$

Where $k_{YN,i}$ and τ_i are Yoon-Nelson rate constant for component i (min^{-1}) and time needed for retaining 50 percent of C_0 for component i concentration (min), respectively. Yoon-Nelson parameters are evaluated from Linear Graph of $\ln[C_i/(C_0 - C_i)]$ versus t , as displayed in Fig. (9(a-d)). Table (5) shows that rate constant values k_{YN} increased with rising flow rate and influent concentration but the 50% breakthrough time τ decreased due to rapid saturation by rising inlet concentration and flow rate [45]. Whereas, τ values of k_{YN} decreased as a volume of bed increased, but τ values increased due to enhancement of a binding site [46-47]. The values of τ_{YN} are similar to experimental results and a good

linear correlation factors (R^2) values of this model are relatively higher (> 0.9), which conclude that fitting of this model for retention of Cs^+ , Sr^{2+} , UO_2^{2+} and Co^{2+} from multicomponent solution onto bentonite-Ca-alginate composite. As illustrated from Tables (4) and (5) it is noticed that good linear correlation factors (R^2) values of Thomas and Yoon-Nelson models therefore, two models are found as well fitted models for investigated ions adsorption system. Finally, bentonite-Ca-alginate composite is an instance of an environmentally friendly and low cost sorbent for hazardous ions. This work concludes that bentonite-Ca-alginate stable up to radiation doses of 100 kGy and could be utilized for discharge of Cs(I) , Sr(II) , U(VI) and Co(II) from aquatic solution.

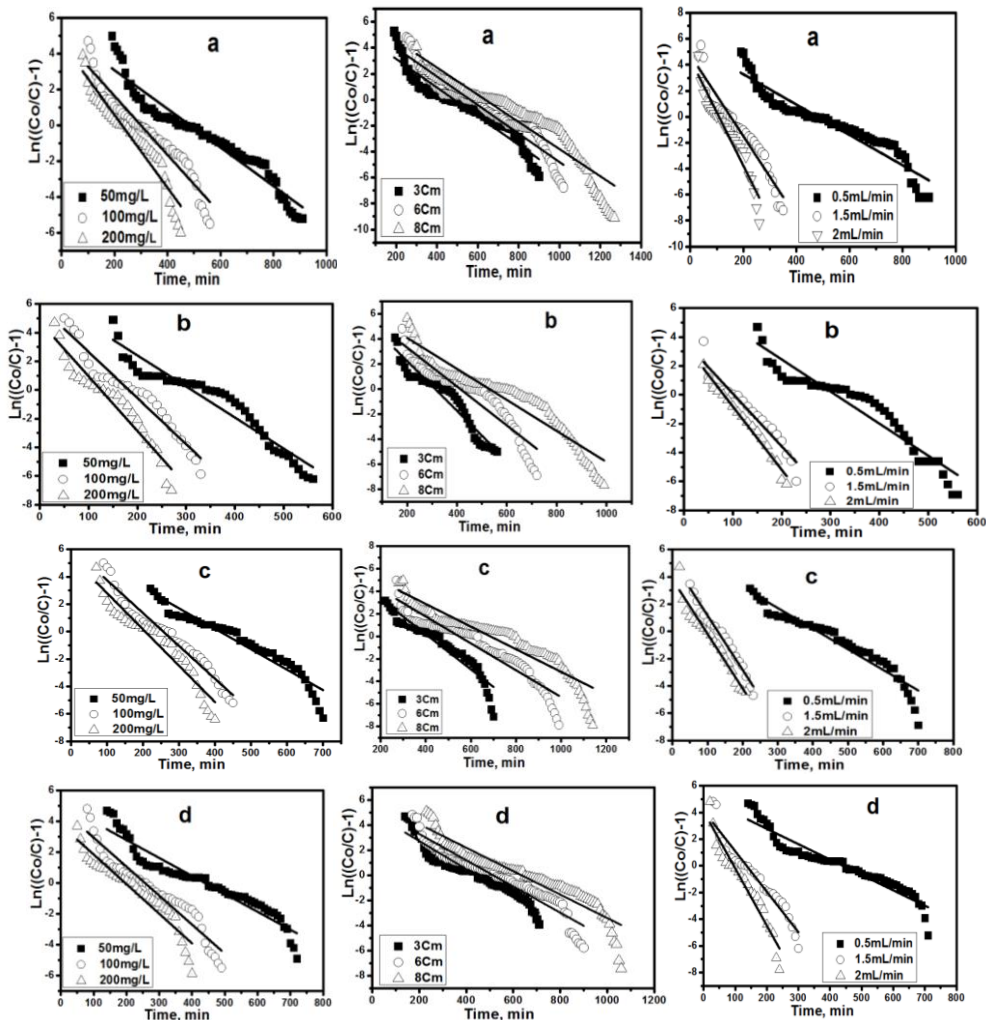


Fig. 8. Thomas model plots for adsorption of (a) Cs^+ , (b) Sr^{2+} , (c) UO_2^{2+} and (d) Co^{2+} by encapsulated bentonite-Ca-alginate at $\text{pH}=5.5$, at different conditions.

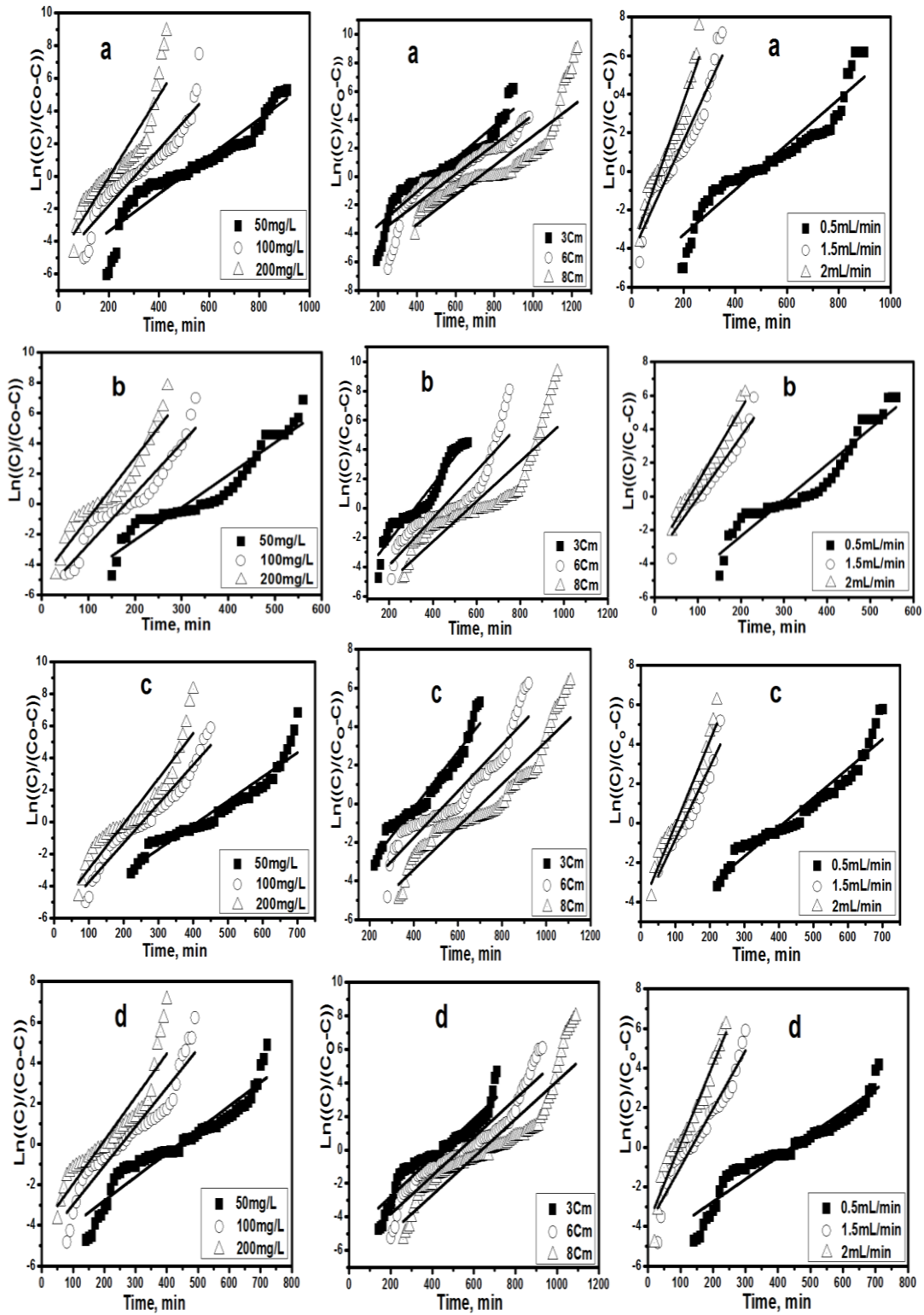


Fig. 9. Yoon-Nelson model plots for adsorption of (a)Cs⁺, (b)Sr²⁺, (c) UO₂²⁺ and (d)Co²⁺ by encapsulated bentonite-Ca-alginate at pH=5.5, at different conditions.

Table 4. Thomas model parameters for the sorption of Cs^+ , Sr^{2+} , UO_2^{2+} and Co^{2+} onto bentonite-Ca-alginate composite beads.

Parameters		Concentration, mg/L			Flow rate, mL/min			Bed depth, cm		
		50	100	200	0.5	1.5	2	3	6	8
Cs^+	K_{Th} , mL/mg/min	0.21	0.16	0.1	0.21	0.63	0.82	0.21	0.2	0.18
	$q_{\text{Th}}(\text{cal.})$, mg/g	12.2	15	22.9	12.2	11.4	10.8	12.2	13.7	17.7
	R^2	0.93	0.93	0.92	0.90	0.92	0.92	0.92	0.92	0.90
Sr^{2+}	K_{Th} , mL/mg/min	0.43	0.32	0.19	0.43	0.73	0.87	0.43	0.3	0.24
	$q_{\text{Th(Cal.)}}$, mg/g	7.75	9.2	12.5	7.75	7.7	7.6	7.75	10.7	13.6
	R^2	0.92	0.94	0.92	0.91	0.92	0.98	0.93	0.88	0.90
UO_2^{2+}	K_{Th} (mL/mg/ min)	0.3	0.23	0.13	0.3	0.78	0.8	0.3	0.24	0.2
	$q_{\text{Th(Cal.)}}$, mg/g	11.4	12.8	20.5	11.4	9.88	9.5	11.4	13.7	17
	R^2	0.93	0.95	0.92	0.92	0.97	0.95	0.91	0.91	0.89
Co^{2+}	K_{Th} (mL/mg/ min)	0.23	0.18	0.1	0.23	0.6	0.8	0.23	0.2	0.18
	$q_{\text{Th(Cal.)}}$, mg/g	11	12.8	19.6	11	10.3	10.2	11	13.5	15.8
	R^2	0.92	0.92	0.91	0.91	0.92	0.93	0.92	0.91	0.89

Table 5. Yoon-Nelson model parameters for the sorption of Cs^+ , S^{2+} , UO_2^{2+} and Co^{2+} onto bentonite-Ca-alginate composite beads.

Parameters		Inlet Concentration (mg/L)			Flow rate (mL/min)			Bed Height (cm)		
		50	100	200	0.5	1.5	2	3	6	8
Cs^+	K_{YN}	0.011	0.017	0.025	0.011	0.029	0.035	0.011	0.01	0.0098
	τ , min	496.5	309.4	227.2	496.5	147.6	106.7	496.5	589	752
	t_{exp} , min	480	300	202	480	160	110	480	570	810
	q_{YN} , mg/g	12.4	15.5	22.7	12.4	11.06	10.07	12.4	14.8	18.8
	R^2	0.90	0.89	0.85	0.90	0.93	0.94	0.90	0.89	0.80
Sr^{2+}	K_{YN}	0.021	0.033	0.039	0.021	0.036	0.044	0.021	0.014	0.0127
	τ , min	317	182.6	126.4	317	102.8	80.7	317	434	510.2
	t_{exp} , min	350	190	130	350	110	80	350	490	640
	q_{YN} , mg/g	7.9	9.13	12.6	7.9	7.7	7.6	7.9	10.9	12.8
	R^2	0.92	0.93	0.92	0.92	0.92	0.97	0.93	0.84	0.82
UO_2^{2+}	K_{YN}	0.015	0.024	0.028	0.015	0.03	0.043	0.015	0.012	0.01
	τ , min	416	257.9	205.4	416	125.3	101.2	416	541	709
	t_{exp} , min	460	280	240	460	140	110	460	610	800
	q_{YN} , mg/g	10.4	12.9	20.5	10.4	9.4	9.2	10.4	13.5	17.7
	R^2	0.92	0.95	0.89	0.94	0.92	0.95	0.95	0.90	0.91
Co^{2+}	K_{YN}	0.012	0.019	0.021	0.012	0.029	0.04	0.012	0.0115	0.0113
	τ , min	425.8	255.6	195.2	425	136.2	96.3	425	531.6	639
	t_{exp} , min	450	260	220	450	130	90	450	560	680
	q_{YN} , mg/g	10.6	12.7	19.5	10.5	10	9.6	10.5	13.3	15.9
	R^2	0.92	0.92	0.86	0.91	0.94	0.95	0.91	0.92	0.86

CONCLUSION

Encapsulated bentonite-Ca-alginate composite beads is considered as low cost sorbent potential for an industrial application and was utilized for dislodge Cs(I), Sr(II), U(VI) and Co(II) from aquatic solution. Appropriate pH value was desired at pH 5.5. ZPC of bentonite-Ca-alginate is approximately 8 as reported with others. Irradiated bentonite-Ca-alginate until 100 kGy has a negligible impact on dislodge the four ions and a structure of bentonite-Ca-alginate. Among the most technological challenges in an adsorption domain was to examine a column performance of bentonite-Ca-alginate composite beads for Cs^+ , Sr^{2+} , UO_2^{2+} and Co^{2+} discharge (multicomponent solution). Column performance for bentonite-Ca-alginate composite beads was examined for removal of Cs^+ , Sr^{2+} , UO_2^{2+} and Co^{2+} from multicomponent solution. These findings conclude that modified bentonite have a good adsorption capacity for discharge of Cs^+ , Sr^{2+} , UO_2^{2+} and Co^{2+} from multicomponent solution with high affinity in an order $\text{Cs}^+ > \text{UO}_2^{2+} > \text{Co}^{2+} > \text{Sr}^{2+}$. Results suggested that initial metal ion concentration, bed depth height and flow rate affect a sorption process. Thomas and Yoon-Nelson models have been successfully used to estimate a breakthrough curve for adsorption, implying that they are very suitable for columns modeling of bentonite-Ca-alginate beads. These finding suggest that modified bentonite has a strong capability to absorb Cs^+ , Sr^{2+} , UO_2^{2+} and Co^{2+} from a high sorption-affinity multicomponent solution with high affinity for sorption of Cs^+ .

REFERENCES

- [1] Yu J, Wang J, Jiang Y. Removal of Uranium from Aqueous Solution by Alginate Beads. *Nucl Eng Technol*. 2017;49(3):534–40.
- [2] Outokesh M, Mimura H, Niibori Y, Tanaka K. Equilibrium and Kinetics of Silver Uptake by Multinuclear Alginate Microcapsules Comprising an Ion Exchanger Matrix and Cyanex 302 Organophosphinic Acid Extractant. *Ind & Eng Chem Res*. 2006;45(10):3633–43.
- [3] Melichová Z, Hromada L. Adsorption of Pb^{2+} and Cu^{2+} Ions from Aqueous Solutions on Natural Bentonite. *Polish J Environ Stud*. 2012;22:457–64.
- [4] Abou-Lilah RA, Rizk HE, Elshorbagy MA, Gamal AM, Ali AM, Badawy NA. Efficiency of bentonite in removing cesium, strontium, cobalt and uranium ions from aqueous solution: encapsulation with alginate for column application. *Int J Environ Anal Chem*. 2020;0(0):1–24.
- [5] Tayyebi A, Khanchi AR, Ghofrani M, Outokesh M. Synthesis and Characterization of a Bentonite-Alginate Microspherical Adsorbent for Removal of Uranyl Ions from Aqueous Solutions. *Sep Sci Technol*. 2010;45:288–98.
- [6] Marczenko Z. Spectrophotometric Determination of Elements. "Ellis Horwood. Ltd., Poland, (1976).
- [7] Felipe ECB, Ladeira ACQ. Separation of zirconium from hafnium by ion exchange. *Sep Sci Technol*. 2018;53(2):330–6.
- [8] Carolin CF, Kumar PS, Saravanan A, Toshiba GJ, Naushad M. Efficient techniques for the removal of toxic heavy metals from aquatic environment: A review. *J Environ Chem Eng*. 2017;5(3):2782–99.
- [9] Jung K-W, Jeong T-U, Choi J-W, Ahn K-H, Lee S-H. Adsorption of phosphate from aqueous solution using electrochemically modified biochar calcium-alginate beads: Batch and fixed-bed column performance. *Bioresour Technol*. 2017 Nov;244(Pt 1):23–32.
- [10] Keshtkar AR, Kafshgari F, Mousavian MA. Binary biosorption of uranium(VI) and nickel(II) from aqueous solution by Ca-pretreated *Cystoseira indica* in a fixed-bed column. *J Radioanal Nucl Chem*. 2012;292(2):501–12.
- [11] Gouran-Orimi R, Mirzayi B, Nematollahzadeh A, Tardast A. Competitive adsorption of nitrate in fixed-bed column packed with bio-inspired polydopamine coated zeolite. *J Environ Chem Eng*. 2018;6(2):2232–40.
- [12] Metwally SS, Hassan HS, Samy NM. Impact of environmental conditions on the sorption behavior of ^{60}Co and $^{152+154}\text{Eu}$ radionuclides onto polyaniline/zirconium aluminate composite. *J Mol Liq*. 2019;287:110941.
- [13] Fiol N, Villaescusa I. Determination of sorbent point zero charge: usefulness in sorption studies. *Environ Chem Lett*. 2009;7(1):79–84.
- [14] Mustafa S, Dilara B, Nargis K, Naeem A, Shahida P. Surface properties of the mixed oxides of iron and silica. *Colloids Surfaces A Physicochem Eng Asp*. 2002;205(3):273–82.
- [15] Badawy NA, El-Baya AA, and Amdeha EJ. Chemical and Pharmaceutical Research. 2015;7(5): 589-98.

- [16] Farooq M, and Ramli A, National Postgraduate Conference. (2011).
- [17] Kim Dong-Su. measurement of point of zero charge of bentonite by solubilization technique and its dependence of surface potential on pH. 8(4):222–7.
- [18] Lantz KE, Yu J, and Wai CMJ, Analytical Chemistry. 1992; 64(3):311–5.
- [19] Anderson Sharon J. A4 - Sposito, Garrison SJA-A. Cesium-Adsorption Method for Measuring Accessible Structural Surface Charge. *Soil Sci Soc Am J.* 1991;v. 55(6):1569–1576–991 v.55 no.6.
- [20] Zhaoyi T, Zhaoya H, Dong Z, Xiaolin W. Structural characterization of ammonium molybdate with different amount of cesium adsorption. *J Radioanal Nucl Chem.* 2014;299(3):1165–9.
- [21] Holdsworth AF, Eccles H, Rowbotham D, Brookfield A, Collison D, Bond G, et al. The Effect of Gamma Irradiation on the Physicochemical Properties of Caesium-Selective Ammonium Phosphomolybdate–Polyacrylonitrile (AMP–PAN) Composites. *Clean Technol.* 2019;1(1):294–310.
- [22] Gournis D, Mantaka-Marketou AE, Karakassides MA, Petridis D. Effect of γ -irradiation on clays and organoclays: a Mössbauer and XRD study. *Phys Chem Miner.* 2000;27(7):514–21.
- [23] Goel J, Kadirvelu K, Rajagopal C, Kumar Garg V. Removal of lead(II) by adsorption using treated granular activated carbon: batch and column studies. *J Hazard Mater.* 2005 Oct;125(1–3):211–20.
- [24] Yunnen C, Ye W, Chen L, Lin G, Jinxia N, Rushan R. Continuous Fixed-Bed Column Study and Adsorption Modeling: Removal of Arsenate and Arsenite in Aqueous Solution by Organic Modified Spent Grains. *Polish J Environ Stud.* 2017 Jun 13;26.
- [25] Luo X, Yuan J, Liu Y, Liu C, Zhu X, Dai X, et al. Improved Solid-Phase Synthesis of Phosphorylated Cellulose Microsphere Adsorbents for Highly Effective Pb²⁺ Removal from Water: Batch and Fixed-Bed Column Performance and Adsorption Mechanism. *ACS Sustain Chem & Eng.* 2017;5(6):5108–17.
- [26] Han R, Wang Y, Zhao X, Wang Y, Xie F, Cheng J, et al. Adsorption of methylene blue by phoenix tree leaf powder in a fixed-bed column: experiments and prediction of breakthrough curves. *Desalination.* 2009;245(1):284–97.
- [27] Singh TS, Pant KK. Experimental and modelling studies on fixed bed adsorption of As(III) ions from aqueous solution. *Sep Purif Technol.* 2006;48(3):288–96.
- [28] Mondal MK. Removal of Pb(II) ions from aqueous solution using activated tea waste: Adsorption on a fixed-bed column. *J Environ Manage.* 2009;90(11):3266–71.
- [29] Zulfadly Z, Mashitah MD, Bhatia S. Heavy metals removal in fixed-bed column by the macro fungus Pycnoporus sanguineus. *Environ Pollut.* 2001;112(3):463–70.
- [30] Futalan CM, Kan C-C, Dalida ML, Pascua C, Wan M-W. Fixed-bed column studies on the removal of copper using chitosan immobilized on bentonite. *Carbohydr Polym.* 2011;83(2):697–704.
- [31] Qaiser S, Saleemi AR, Umar M. Biosorption of lead from aqueous solution by *Ficus religiosa* leaves: Batch and column study. *J Hazard Mater.* 2009;166(2):998–1005.
- [32] Taty-Costodes VC, Fauduet H, Porte C, Ho Y-S. Removal of lead (II) ions from synthetic and real effluents using immobilized *Pinus sylvestris* sawdust: Adsorption on a fixed-bed column. *J Hazard Mater.* 2005;123(1):135–44.
- [33] Jerold M, Joseph D, Patra N, Sivasubramanian V. Fixed-bed column studies for the removal of hazardous malachite green dye from aqueous solution using novel nano zerovalent iron algal biocomposite. *Nanotechnol Environ Eng.* 2016;1(1):8.
- [34] Kuppusamy V, Jegan J, Palanivelu K, Velan M. Copper removal from aqueous solution by marine green alga *Ulva reticulata*. *Electron J Biotechnol.* 2004;7:47–54.
- [35] Han R, Wang Y, Zou W, Wang Y, Shi J. Comparison of linear and nonlinear analysis in estimating the Thomas model parameters for methylene blue adsorption onto natural zeolite in fixed-bed column. *J Hazard Mater.* 2007;145(1):331–5.
- [36] Kundu S, Gupta AK. Analysis and modeling of fixed bed column operations on As(V) removal by adsorption onto iron oxide-coated cement (IOCC). *J Colloid Interface Sci.* 2005;290(1):52–60.
- [37] Thomas HC. Heterogeneous Ion Exchange in a Flowing System. *J Am Chem Soc.* 1944;66:1664–6.
- [38] Aksu Z, Gönen F. Biosorption of phenol by immobilized activated sludge in a continuous packed bed: prediction of breakthrough curves. *Process Biochem.* 2004;39(5):599–613.
- [39] Padmesh TVN, Vijayaraghavan K, Sekaran G, Velan M. Biosorption of Acid Blue 15 using fresh water macroalgae *Azolla filiculoides*: Batch and column studies. *Dye Pigment.* 2006;71(2):77–82.

- [40] Xiong C, Li Y, Wang G, Fang L, Zhou S, Yao C, et al. Selective removal of Hg(II) with polyacrylonitrile-2-amino-1,3,4-thiadiazole chelating resin: Batch and column study. *Chem Eng J.* 2015;259:257–65.
- [41] Nouri H, Ouederni A. Modeling of the Dynamics Adsorption of Phenol from an Aqueous Solution on Activated Carbon Produced from Olive Stones. *Int J Chem Eng Appl.* 2013;254–61.
- [42] Ji F, Li C, Xu J, Liu P. Dynamic adsorption of Cu(II) from aqueous solution by zeolite/cellulose acetate blend fiber in fixed-bed. *Colloids Surfaces A Physicochem Eng Asp.* 2013;434:88–94.
- [43] Ahmad AA, Hameed BH. Fixed-bed adsorption of reactive azo dye onto granular activated carbon prepared from waste. *J Hazard Mater.* 2010;175(1):298–303.
- [44] Nyong EE, Olsson RK. A paleoslope model of Campanian to lower Maestrichtian foraminifera in the North American basin and adjacent continental margin. *Mar Micropaleontol.* 1984;8(6):437–77.
- [45] Recepoglu YK, Kabay N, Ipek IY, Arda M, Yüksel M, Yoshizuka K, et al. Packed bed column dynamic study for boron removal from geothermal brine by a chelating fiber and breakthrough curve analysis by using mathematical models. *Desalination.* 2018;437:1–6.
- [46] Liu D, and Sun DJ, Environmental Engineering and Science. 2012;29: 461–5.
- [47] Aziz ASA, Manaf LA, Man HC, Kumar NS. Column dynamic studies and breakthrough curve analysis for Cd(II) and Cu(II) ions adsorption onto palm oil boiler mill fly ash (POFA). *Environ Sci Pollut Res.* 2014;21(13):7996–8005.

نمذجة الإمتراز الديناميكي لبعض العناصر الخطيرة من محلول مائي على حبيبات كالسيوم الجينات البنتونيت

ريهام عبدالكريم ابراهيم أبوليلاه*-هدي السيد رزق*-مصطفى عبد المنعم الشوريجي*-عزة محمد جمال- امال محمد علي*-نجوى عبدالفتاح بدوي

قسم الكيمياء- كلية العلوم (بنات)- جامعة الأزهر
*قسم تكنولوجيا الوقود النووي- مركز المعلم الحار- هيئة الطاقة الذرية

يهدف هذا العمل الى معالجة النفايات المشعة عن طريق استخدام متراكب البنتونيت مع الألجينات لإزالة بعض الأيونات الخطيرة (السيزيوم ، الإسترانتشيوم ، اليورانيوم ، الكوبالت). متراكب الجينات البنتونيت تم تحضيره سابقاً وعمل دراسة الخواص الشكلية له مثل دراسة التشكل السطحي و طيف الأشعة تحت الحمراء للمتراكب حيث تبين تحمل الألجينات في المتراكب المحضر. اشتمل هذا البحث على دراسة الشحنة الصفرية للألجينات البنتونيت باستخدام 0.1 مولار من كافوريد الصوديوم عند تركيزات مختلفة من أيون الهيدروجين.. . وقد تبين أن قيمة الشحنة الصفرية للألجينات البنتونيت التي يكون عندها السطح لا يحمل أي شحنة موجبة أو سالبة عند($pH=8$). تم دراسة تأثير تركيز أيون الهيدروجين على إمتراز أيونات (السيزيوم ، الإسترانتشيوم ، اليورانيوم ، الكوبالت) بواسطة الألجينات البنتونيت في مدي 7-1 ووجد انها علاقية طردية.

لقد تم دراسة كفاءة الألجينات البنتونيت في إزالة هذه الأيونات وذلك بعد تعريضها لجرعات إشعاعية مختلفة من 100-25 كيلو جrai وتم عمل تحليل طيف الأشعة تحت الحمراء لها بعد تعريضها للإشعاع وتبين أنها محافظة بنفس المجموعات الوظيفية الخاصة بها ولم يحدث أي تغيير في تركيبها بعد الإشعاع كما تبين أن سعة الألجينات البنتونيت تزيد زيادة طفيفة بزيادة الجرعات الإشعاعية المعرضة لها مايدل على ثبات الألجينات البنتونيت لجرعات إشعاعية تصل إلى 100 كيلو جrai.

تم دراسة تأثير العوامل المختلفة على أداء عمود الإمتراز مثل تأثير تركيز الأيونات عند تركيزات مختلفة من أيونات (السيزيوم ، الإسترانتشيوم ، اليورانيوم ، الكوبالت) وهي (50,100,200 مجم/لتر لكل عنصر و عند أرتفاعات مختلفة للعمود (3,6,8) سم وأيضا عند معدلات تدفق مختلفة من (0.5,1.5,2) مللي/ دقيقة و ذلك من محلول متعدد المكونات. وقد تبين أنه بزيادة تركيز الأيونات يقل معدل الإزالة وتزيد سعة الأمتراز بينما بزيادة معدلات التدفق لهذه الأيونات يقل من معدل الإزالة و سعة الأمتراز معا. كما تبين أنه بزيادة ارتفاع العمود تزيد سعة الأمتراز ويزيد الحجم المطلوب لهذه العناصر.

تم تطبيق نماذج الإمتراز الديناميكي لوصف العوامل الكيناتيكية للإمتراز في العمود وهما نموذجا توماس و يوون نيلسون وأظهرت النتائج أن هناك تطابق مع هذين النموذجين وأن هناك توافق بين البيانات المسحوبة والتجريبية.